ACS OMEGA

http://pubs.acs.org/journal/acsodf

Article

Application of Allometric Scaling to Nanochelator Pharmacokinetics

Gregory Jones, Lingxue Zeng, and Jonghan Kim*

Cite This: *ACS Omega* 2023, 8, 27256−27263

Read Online

ACCESS | Metrics & More | Article Recommendations | Supporting Information

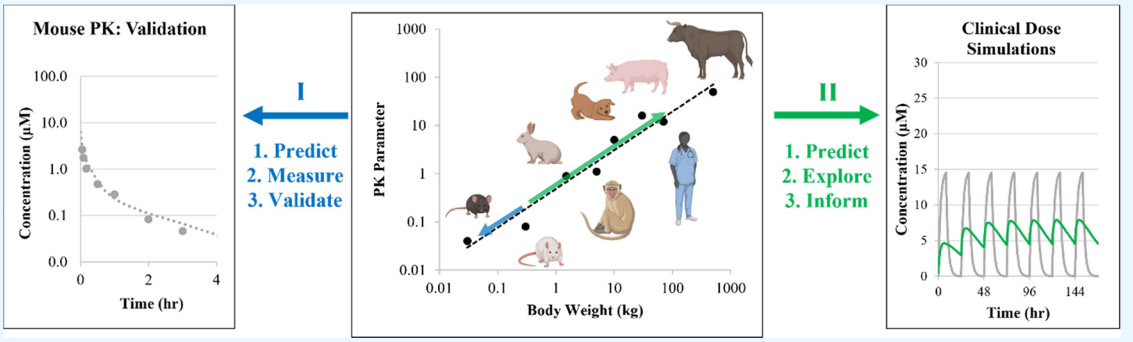

ABSTRACT: Deferoxamine (DFO) is an effective FDA-approved iron chelator; however, its use is considerably limited by off-target toxicities and an extremely cumbersome dose regimen involving daily infusions. The recent development of a deferoxamine-based nanochelator (DFO-NP) with selective renal excretion has shown promise in ameliorating iron overload and associated physiological complications in rodent models with a substantially improved safety profile. While the dose- and administration route-dependent pharmacokinetics (PK) of DFO-NPs have been recently characterized, the optimized PK model was not validated, and the prior studies did not directly address the clinical translatability of DFO-NPs into humans. In the present work, these gaps were addressed by applying allometric scaling of DFO-NP PK in rats to predict those in mice and humans. First, this approach predicted serum concentration−time profiles of DFO-NPs, which were similar to those experimentally measured in mice, validating the nonlinear disposition and absorption models for DFO-NPs across the species. Subsequently, we explored the utility of allometric scaling by predicting the PK profile of DFO-NPs in humans under clinically relevant dosing schemes. These in silico efforts demonstrated that the novel nanochelator is expected to improve the PK of DFO when compared to standard infusion regimens of native DFO. Moreover, reasonable formulation strategies were identified and discussed for both early clinical development and more sophisticated formulation development.

INTRODUCTION

Iron is an essential metal for proper physiological function;[1] however, labile iron can produce reactive oxygen species which can lead to severe organ damage after sustained exposure.[2] The abnormal accumulation of iron in the liver, pancreas, and heart, can cause a range of health issues including diabetes, liver cirrhosis, cardiac arrhythmias, and even death from cardiac failure.[2,3] Anemic and transfusion-associated iron overload disorders are treated by iron chelation therapy (ICT), with 3 small molecule iron chelators currently approved for this indication: deferoxamine, deferiprone, and deferasirox.[4,5] While each approved chelator has been shown to ameliorate iron overload, these existing ICTs cannot meet their full therapeutic potential due to dose-limiting toxicities and poor patient compliance caused by potentially severe side effects.[5]

Nanochelators are a class of novel iron chelators that have received significant attention in the last decade due to their ability to extend chelator half-life and reduce off-target chelator distribution which can be associated with toxicities. Readers are encouraged to consult the works of Hamilton and Kizhakkedathu[6] and Jones et al.[7] for a recent review of advances in nanochelator technologies. In particular, Kang et al.[8] have reported on a novel, renal selective DFO-conjugated nanoparticle (DFO-NP; nanochelator) prepared by conjugating DFO to ε-poly-lysine (EPL). This promising nanochelator has demonstrated robust iron chelation in vivo and an improved safety profile compared to native DFO.[8,9]

To facilitate the clinical translation of this novel therapeutic, the pharmacokinetic profile of DFO-NP should be fully characterized. We have previously characterized the pharmacokinetics of DFO-NPs in rats using model-independent noncompartmental analysis (NCA) at multiple relevant therapeutic doses after IV and SC administration.[10] The outcomes of these

Received: April 14, 2023
Accepted: June 22, 2023
Published: July 18, 2023

Table 1. Scaling of Model-Based PK Parameters in Rodents for DFO-NP Disposition

parameter (*units*)	parameter description	allometric exponent	rat value[a]	mouse value[b]
body mass (kg)	animal body mass	N/A	0.350	0.035
V_1 (L)	volume of central compartment	1	0.0169	0.00169
V_2 (L)	volume of peripheral compartment	1	0.0486	0.00486
V_3 (L)	volume of tubular compartment	1	2.53×10^{-3}	2.53×10^{-4}
K_{12} (h^{-1})	intercompartmental rate constant (central to peripheral)	−0.25	1.40	2.50
K_{21} (h^{-1})	intercompartmental rate constant (peripheral to central)	−0.25	0.489	0.869
K_{13} (h^{-1})	intercompartmental rate constant (central to tubular)	−0.25	7.33	13.0
$V_{max\_recycle}$ (μmol/h)	maximal rate of capacity-limited DFO-NP transport from tubular to central compartment	0.75	5.58	0.992
$K_{m\_recycle}$ (μM)	DFO-NP concentration in tubular compartment yielding $^1/_2$ $V_{max\_recycle}$	N/A	464	464
K_{30} (h^{-1})	apparent elimination rate constant	−0.25	2.56	4.58

[a]Model-based parameters calculated from experimentally measured data.[11] [b]Allometry-based predicted values; N/A, not applicable.

studies indicated that DFO-NPs show nonlinear PK after both IV and SC administration, and the results suggested that the disposition of nanochelators was governed by a saturable elimination process. Furthermore, we applied mechanism-based pharmacokinetic modeling to characterize the saturable absorption and disposition of DFO-NPs and to develop a model that accounted for the observed nonlinearity in these processes.[11] While this mechanism-based model adequately and quantitatively described the nonlinear pharmacokinetics of DFO-NPs in rats, its utility of predicting nanochelator PK in other species remained to be evaluated. To directly address the clinical translatability of this novel nanochelator into humans, in the present study we have applied allometric scaling to the mechanism-based PK model. We first validated our model-based scaling approach in mice and then evaluated clinical dosing schemes in humans to provide guidance for clinical development. Lastly, based on the results, we provided reasonable formulation strategies that were identified and discussed for both early clinical development and more sophisticated formulation development.

MATERIALS AND METHODS

Allometric Scaling of Model-Based PK Parameters. Traditional allometric scaling[12] was used to calculate the model-based PK parameters for DFO-NPs in both mice and humans using the model structures and model-based parameters determined in rats.[11] In this approach, the PK parameter (Y) is related to body weight (W) using the power law equation:

$$Y = aW^b \quad (1)$$

where a is the allometric coefficient and b is the allometric exponent.

Parameters were scaled using body weight estimates of 35 g for CD-1 mice, 350 g for Sprague Dawley rats, and 70 kg for humans. Allometric exponents were chosen as follows: $b = 1$ was implemented for volumes of distribution, $b = 0.75$ was implemented for clearance and V_{max}, and $b = -0.25$ was implemented for all rate constants.[13,14]

Simulation of Predicted PK Profile. Simulations were performed using the SimBiology Model Analyzer application within the MATLAB software (Version #2021a). Scaled kinetic parameters for mice or humans were used to simulate the disposition of DFO-NPs after IV or SC administration. For mouse simulations, doses were matched to the experimental conditions. For human simulations, single-dose amounts were matched to the equivalent concentration of native DFO used in published clinical data.[15,16] For exploratory human dose scouting, dose amount and dose frequency were varied as simulation inputs. For all simulations, the simulation time was adjusted to encompass the appropriate timeframe, generally 4−8 h for mouse simulations, 96 h for single-dose human simulations, 168 h for repeat dose simulations, and 30 days for sustained release simulations. Simulated data were exported from the MATLAB workspace and plotted in Microsoft Excel.

Comparison of Predicted and Measured PK Profiles in Mice for Model Validation. Published pharmacokinetic data from our lab for DFO-NPs administered IV in CD-1 mice at doses of 0.3 and 2 μmol/kg were used in this study.[8] To support model validation, the PK of DFO-NPs administered SC in mice was determined experimentally (Supporting Information). The predicted and measured PK profiles were first evaluated by visual inspection to qualitatively assess the alignment in the shapes of the curves. When robust plasma measurements were available (i.e., multiple animals per timepoint with mean ± SD), the coefficient of determination (R^2) was calculated to quantitatively assess how accurately the predicted outcomes aligned with the measured results.

RESULTS

Interspecies Scaling and Model Validation for Intravenous Administration. To examine if our nonlinear PK model adequately predicts the PK profile of DFO-NP in other species, we first scaled down model-based PK parameters from rat to mouse (Table 1). Briefly, we applied the previously optimized 3-compartment mammillary disposition model with saturable reabsorption and elimination from the "tubular" compartment (Figure 1A;[11]) and simulated the concentration−time profile of DFO-NPs in mice for 4 h after IV administration of 0.3 and 2 μmol/kg doses (Figure 1). The predicted serum concentration−time profile of the low dose (0.3 μmol/kg) aligned well with the measured data qualitatively via visual inspection (Figure 1B) and the goodness of fit was confirmed through quantitative analysis as evidenced by the value of $R^2 = 0.8347$. The predicted concentration−time profile of the high dose (2 μmol/kg) aligned reasonably with the measured data (Figure 1C) based on an R^2 value of 0.5704 when analyzed for the goodness of fit.

For more precise prediction, the model may require adjustments to the reabsorption process, for example reducing the value of $K_{m\_recycle}$ to account for the difference in terminal phase predictions between the low and high dose (i.e., having reabsorption saturate easier and lower predicted concentrations

https://doi.org/10.1021/acsomega.3c02570
ACS Omega 2023, 8, 27256−27263

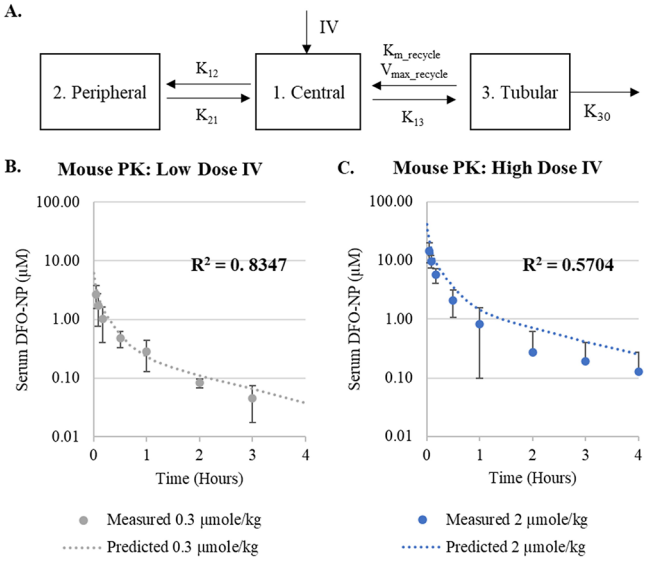

Figure 1. Comparison of predicted and measured DFO-NP PK after IV administration in CD-1 mice. (A) Three-compartment mammillary model with saturable reuptake and elimination from tubular compartment.[11] (B) Comparison of measured and predicted concentration−time profile after 0.3 μmol/kg IV dose. (C) Comparison of measured and predicted concentration−time profile after 2 μmol/kg IV dose.

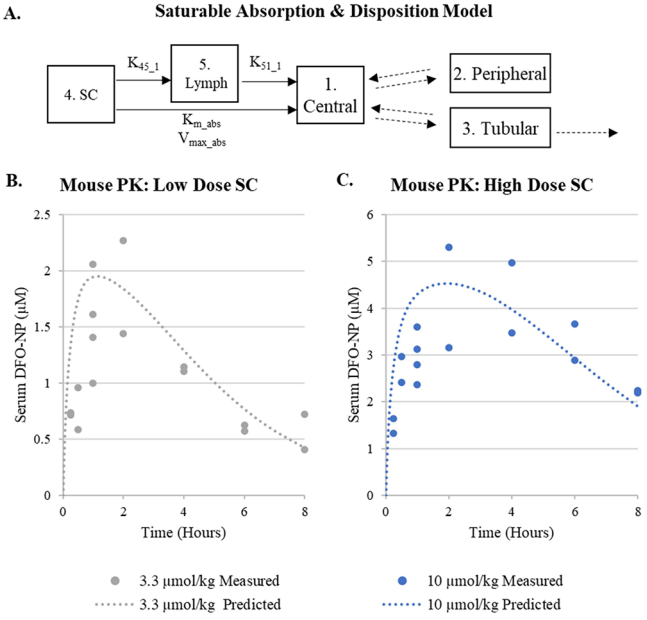

Figure 2. Comparison of predicted and measured DFO-NP PK after SC administration in CD-1 mice. (A) Structure of compartment-based model with saturable absorption into central compartment, saturable reabsorption from tubular compartment into central compartment, and elimination from tubular compartment.[11] (B) Comparison of the measured and predicted concentration−time profiles after a 3.3 μmol/kg SC dose shows an overestimation of early (<1 h) absorption kinetics. (C) Comparison of the measured and predicted concentration−time profiles after a 10 μmol/kg SC dose shows an overestimation of early (<1 h) absorption kinetics.

at high dose). Mechanistically, this could be due to potential species-specific differences in the saturable reabsorption of DFO-NPs, including different density and affinity of receptors that are responsible for the uptake of nanoparticle in the kidney and would require additional experimental data to discern. The predictive accuracy may also be improved with DFO-NP-specific allometric scaling exponents, which will also require additional PK studies in multiple species.

Interspecies Scaling and Model Validation for Subcutaneous Administration. Serum DFO-NP concentrations were quantified for 8 h following SC administration of 3.3 and 10 μmol/kg doses in mice. The SC bioavailability, as calculated by the ratio of the $AUC_{0-\infty}$ for the measured SC groups to the simulated IV groups with matched doses, was determined to be 0.90 for the 3.3 μmol/kg dose and 1.0 for the 10 μmol/kg dose. The model-based PK parameters for the previously optimized saturable SC absorption model (Figure 2A[11]) were scaled down from rat to mouse (Table 2) and the serum concentration−time profile of DFO-NPs was simulated for 8 h. The predicted serum concentration−time profiles of both 3.3 and 10 μmol/kg doses (Figure 2B,C) show a consistent overestimation of drug concentration at very early timepoints (<1 h; see the Discussion section).

Interspecies Scaling and Single-Dose Human PK Prediction. To gain translational insights, model-based PK parameters were scaled up from rats to humans (Table 3) and DFO-NP disposition was simulated (Figure 3) for SC administration and compared to published PK data on native DFO given as a SC infusion in a clinical setting.[16] Since the SC bioavailability of large molecules is difficult to predict in humans[17,18] and since DFO-NPs showed a dose-dependency on bioavailability, all of the human simulations used a conservative bioavailability estimate of 50%, which was the lowest measured value from the animal studies.[10] In the first simulation scenario, the dose of DFO_5-NPs (12.3 μmol/kg as NP or 61 μmol/kg as DFO) was set to the equivalent clinical dose of native DFO on a molar basis (40 mg/kg, or 61 μmol/kg total dose). The predicted PK profile of DFO-NPs at the equimolar dose (Figure 3A) demonstrated a substantial increase in drug exposure, with the DFO-NPs achieving a higher C_{max} and substantially increasing the duration of drug exposure. Quantitatively, the equimolar dose of DFO-NP increased the cumulative exposure to DFO by nearly 4× based on the AUC of the predicted PK profile, which has positive implications for therapeutic efficacy.

In the second simulation scenario, the DFO-NP dose (3.1 μmol/kg) was adjusted to give an equivalent AUC to the clinical regimen of native DFO. The predicted PK profile of DFO-NP at this dose (Figure 3B) had a 2−3× lower C_{max} and a longer duration of exposure, which suggests that the improved PK profile of DFO-NPs can enhance the dosing efficiency, with a nearly 4-fold lower dose needed on a molar basis. Importantly, both simulations were conducted with a bolus SC dose, whereas the published data were for a lengthy and cumbersome infusion. This has positive implications for ease of administration in a clinical setting and at home for routine treatment.

In Silico Dose Scouting: Simulations of Possible Clinical Dosing Schemes. Model-based simulations (Figure 4) were next used to assess different dose schemes that could be feasible for early clinical development. Native DFO PK was simulated for daily clinical infusions using published PK parameters[15] that were determined by fitting a model to the same published clinical infusion data used as a comparator for the single-dose simulations (Figure 3). The first clinical DFO-NP scenario tested was a 2.5 μmol/kg SC bolus administered once daily (Figure 4A). This regimen was predicted to give a favorable PK profile, with a narrow range of steady-state concentrations reached after 3 days of dosing. The narrow range of predicted DFO-NP concentrations at steady-state contrasted

https://doi.org/10.1021/acsomega.3c02570
ACS Omega 2023, 8, 27256−27263

Table 2. Scaled Model-Based PK Parameters in Rodents for DFO-NP Absorption

parameter (units)	parameter description	allometric exponent	rat value[a]	mouse value[b]
body mass (kg)	animal body mass	N/A	0.350	0.035
V_4 (L)	SC compartment volume	1	0.0157	0.00157
K_{45_1} (h^{-1})	first-order rate constant for transport from SC to Lymph compartments	−0.25	0.0302	0.0538
K_{51_1} (h^{-1})	first-order absorption rate constant from lymph to central compartment	−0.25	1.27×10^{-4}	2.25×10^{-4}
V_{max_abs} (μmol/h)	maximum absorption rate of DFO-NP from SC to central compartment	0.75	0.510	0.0906
K_{m_abs} (μM)	concentration of DFO-NP in SC space giving $^1/_2$ maximal absorption rate	N/A	174	174

[a]Model-based parameters calculated from experimentally measured data. [b]Allometry-based predicted values; N/A, not applicable.

Table 3. Scaled Model-Based PK Parameters for DFO-NPs in Humans

parameter (units)	parameter description	allometric exponent	rat value[a]	human value[b]
body mass (kg)	animal body mass	N/A	0.350	70
V_1 (L)	volume of central compartment	1	0.0169	3.39
V_2 (L)	volume of peripheral compartment	1	0.0486	9.73
V_3 (L)	volume of tubular compartment	1	0.00253	0.506
V_4 (L)	SC compartment volume	1	0.0157	3.14
K_{45_1} (h^{-1})	first-order rate constant for transport from SC to lymph compartments	−0.25	0.0302	0.00804
K_{51_1} (h^{-1})	first-order absorption rate constant from lymph to central compartment	−0.25	1.27×10^{-4}	3.38×10^{-5}
V_{max_abs} (μmol/h)	maximum absorption rate of DFO-NP from SC to central compartment	0.75	0.510	27.1
K_{m_abs} (μM)	concentration of DFO-NP in SC space giving $^1/_2$ maximal absorption rate (V_{max_abs})	N/A	174	174
K_{12} (h^{-1})	intercompartmental rate constant (central to peripheral)	−0.25	1.40	0.373
K_{21} (h^{-1})	intercompartmental rate constant (peripheral to central)	−0.25	0.489	0.130
K_{13} (h^{-1})	intercompartmental rate constant (central to tubular)	−0.25	7.33	1.95
$V_{max\_recycle}$ (μmol/h)	maximal rate of capacity-limited DFO-NP reabsorption from tubular to central compartment	0.75	5.58	297
$K_{m\_recycle}$ (μM)	DFO-NP concentration in tubular compartment yielding $^1/_2$ $V_{max\_recycle}$	N/A	464	464
K_{30} (h^{-1})	apparent elimination rate constant	−0.25	2.56	0.685

[a]Model-based parameters calculated from experimentally measured data. [b]Allometry-based predicted values; N/A, not applicable.

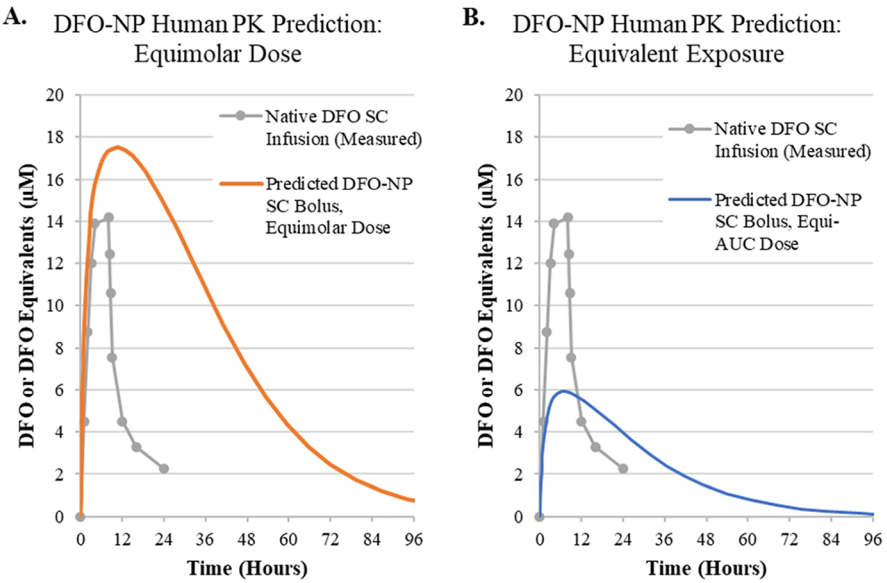

Figure 3. Comparison of the published native DFO PK and the predicted DFO-NP PK in humans. (A) Predicted PK profile of an equimolar DFO-NP dose (12.3 μmol/kg) demonstrates a slight increase in C_{max} and a substantial increase in the extent and duration of exposure (i.e., AUC). (B) When the DFO-NP dose (3.1 μmol/kg) was adjusted to give the same total exposure (i.e., the "Equi-AUC Dose"), the predicted PK profile showed a reduction in C_{max} and an increase in the duration of exposure. (A, B) Native DFO PK data (gray curve) were published for an 8 h SC infusion of 5 mg/kg/h delivered in a clinical setting to thalassemic patients.[16]

starkly with the large peak-to-trough variations seen in the measured DFO group, which resulted in approximately 8−10 h per day with negligible DFO on board.

The second clinical DFO-NP scenario evaluated was a 25 μmol/kg SC bolus administered once weekly (Figure 4B). This regimen was predicted to substantially increase drug exposure within the first 24 h, followed by sustained exposure to the drug

https://doi.org/10.1021/acsomega.3c02570
ACS Omega 2023, 8, 27256−27263

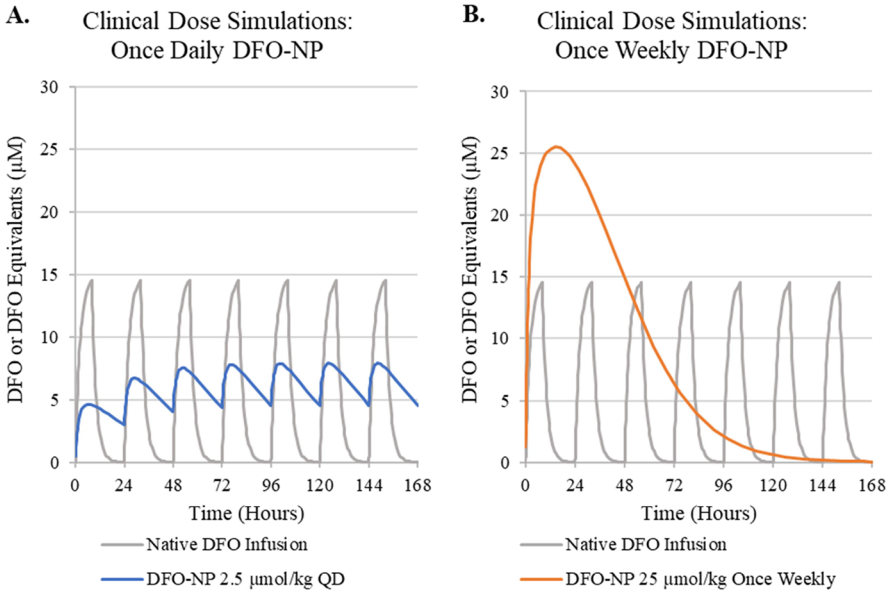

Figure 4. Simulation-based scouting of clinical administration schemes for DFO-NPs compared to established clinical infusion of DFO. (A, B) Simulations of native DFO PK showed that the clinical dose regimen of an 8 h SC infusion at 5 mg/kg/h resulted in large peak-to-trough variations that led to 8−10 h per day with negligible DFO exposure. (A) Model-based simulations suggested that DFO-NPs administered as a daily 2.5 μmol/kg SC injection would reach steady-state concentrations after 3 doses and maintain a narrow concentration window with a minimal peak-to-trough variation. (B) Model-based simulations suggested that DFO-NPs could be administered once weekly as a 25 μmol/kg large-volume SC bolus to rapidly chelate iron in the first 24 h with an additional 72−96 h of robust chelator exposure.

for approximately 96−120 h. While drug exposure was not as continuous as that seen in the 2.5 μmol/kg QD condition, once weekly dosing would provide a tremendous benefit to patient convenience and could conceivably improve chelation efficacy by rapidly chelating iron early on to generate sink conditions for further chelation.

Further simulations were caried out to explore the feasibility of monthly dosing of 75 μmol/kg DFO-NPs, which could be enabled through the development of sustained release formulations (Figure 5). First, a bolus dose of DFO-NPs was simulated (Figure 5A), which predicted a sharp rise and fall in DFO-NP concentration with no meaningful exposure expected after 10 days. Next, the rate constants governing DFO-NP absorption (i.e., K_{45_1} and V_{max_abs}) were systematically decreased by 2.5× (Figure 5B), 5× (Figure 5C), or 10× (Figure 5D). The decreases in the absorption rate progressively extended the duration of drug exposure, and an ideal profile for monthly dosing was observed for the condition with a 5× decrease. This suggests that a formulation that substantially slowed the release of DFO-NP, with minimal burst and near zero-order kinetics, could give favorable PK for monthly dosing.

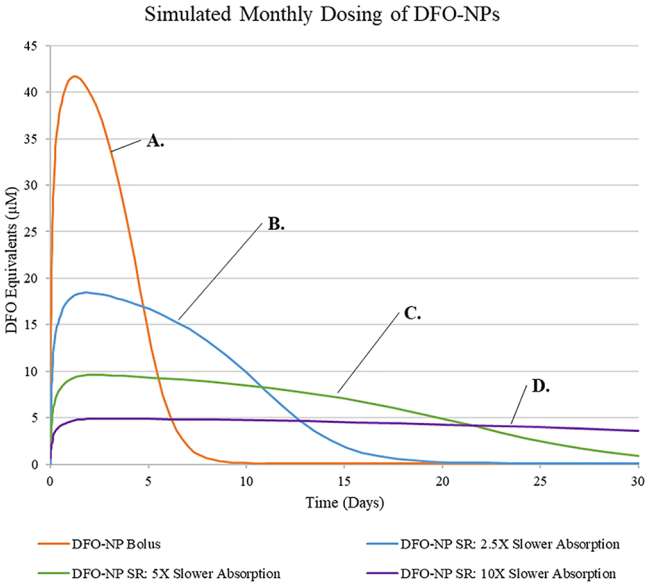

Figure 5. Simulations of theoretical sustained release (SR) DFO-NP formulations for monthly administration of 75 μmol/kg. (A) Simulation of SC bolus dose of DFO-NP shows only 10 days of exposure. (B) Simulation of SC dose with 2.5× slower absorption increases the duration of exposure to nearly 20 days. (C) Simulation of SC dose with 5× slower absorption retains early T_{max} and sustains exposure for 30 days. (D) Simulation of SC dose with 10× slower absorption increases exposure well beyond 30 days.

DISCUSSION

Allometric scaling and model-based simulations were used to validate the PK model governing the absorption of disposition of DFO-NP and to subsequently predict human PK under various conditions. The validation studies had to be conducted in mice due to practical limitations on conducting the studies in rats (e.g., the inability to give novel doses that could be robustly detected and adequately differentiated from the data used to generate the model parameters). The predicted disposition of DFO-NPs administered via IV injection matched well with previously published PK data, especially for the lower dose. While the high dose slightly overpredicted the DFO-NP concentration, the predicted concentrations were within the standard deviation of the measured data, which was a favorable outcome.

Subsequently, the validity of the saturable absorption model was evaluated by comparing model predictions to new PK data generated for model validation. Unexpectedly, the model overpredicted DFO-NP concentrations in the early absorption phase (<1 h), but aligned well with later measurements. This

https://doi.org/10.1021/acsomega.3c02570
ACS Omega 2023, 8, 27256−27263

outcome suggests that the model underpredicted the extent of lymphatic involvement in the mouse, which resulted in the predicted T_{max} occurring sooner than the measured T_{max}. This finding is likely due to the substantial change in the dosing solution used between the model building (i.e., rat) and model validation (i.e., mouse) studies. For the model validation study, mice were dosed using a 10× larger volume of drug solution at a 10× lower concentration than that used in the original rat studies, a practical change that was needed to ensure the dose could be accurately administered. Since lymph formation is determined almost exclusively by interstitial pressure,[19] the increase in the injection volume is expected to increase lymphatic uptake by increasing the hydrostatic pressure in the SC space.[20,33] The change in concentration may also impact the direct absorption pathway which is concentration-dependent. Further evaluation of the impact of dosing solution on absorption kinetics is merited and should be incorporated directly into the model.

Allometric scaling was also used to predict the human PK of DFO-NPs in an effort to understand the viability of SC administration for first-in-human (FIH) clinical studies, and to provide some guidance for clinical formulation development. The preliminary simulations matched the dose of DFO-NPs to the clinical dose of native DFO, using an equivalent molar amount or a dose yielding an equivalent exposure by AUC. In both cases, simulations of a single SC bolus of DFO-NPs demonstrated substantial PK benefits without the need for a cumbersome 8 h infusion. Dosing of an equivalent amount of DFO-NPs substantially increased the amount of drug exposure by 4×, and importantly increased the duration of drug exposure at μM concentrations by 4×, an important benchmark when one considers serum iron concentrations are generally in the μM range.[1] When the dose was tailored to give an equivalent total exposure, DFO-NPs still extended the duration of exposure at μM concentrations while using a nearly 5× lower dose. In both cases, increasing the duration of drug exposure is expected to improve the therapeutic efficacy, since iron needs to mobilize from tissue stores into the systemic circulation. Accomplishing this with a bolus dose bodes well for clinical uptake in this patient population.

After demonstrating the benefits of SC bolus administration of DFO-NPs in a clinical setting, additional simulations were used to develop strategies for clinical formulation development. In the first scenario, we explored the impact of once daily dosing and identified 2.5 μmol/kg as a suitable dose that gives a desirable predicted PK profile. This dose is the upper limit for a reasonable formulation for SC administration, based on the key constraint of a maximum 2−3 mL SC injection volume in humans[17] and a feasible DFO-NPs solution concentration of approximately 50 mM (or 500 mg/mL). While this is feasible due to the high aqueous solubility of the nanochelator, the viscosity would need to be managed to <20 cps to ensure easy and painless administration,[21] which could be done through viscosity reduction strategies employed for biotherapeutic formulations.[17,18] The DFO-NP viscosity will also be improved by removing the NIR fluorophore for clinical formulation development, as this contributes to approximately 1/8th of the total molecular weight. Moreover, these injectability challenges will be lessened if the actual human bioavailability of DFO-NP is greater than the conservative estimate of 50% used in these simulations. In this context, it may be prudent for early FIH studies to proceed with subdivided injections (e.g., 2× 1.5 mL injections at 1/2× concentration) until the actual bioavailability can be determined and an optimized formulation developed. This dosing strategy will also enable self-administration by patients, which can improve convenience and decrease costs by not requiring the involvement of a healthcare professional.

A second development strategy was to explore conditions that facilitate once-weekly dosing, which can substantially improve patient convenience, and therefore compliance and therapeutic outcomes. The simulated 25 μmol/kg SC bolus dose gave adequate DFO-NP exposure for 4−5 days, which was comparable to the cumulative weekly exposure of native DFO infused daily. The large dose volume needed for this dose amount (25−30 mL) could be facilitated by large-volume injection technologies such as on-body pumps that can deliver up to 50 mL.[17] Alternatively, this dose could be delivered in conjunction with the Halozyme ENHANZE technology, which enables large-volume injections. This approach uses a recombinant human hyaluronidase (rHuPH20) to transiently remodel the subcutaneous extracellular matrix and enable substantially larger injections that can exceed 500 mL.[22,23] This technology is FDA-approved and is used in a number of marketed products including HYQVIA (immunoglobulin), Herceptin SC (trastuzumab), and Rituxan HYCELA (rituximab).[23]

The final development strategy was to explore absorption profiles that would enable once-a-month dosing of DFO-NPs, which is a highly desirable dose schedule that aligns with typical blood infusion regimens used to treat the underlying pathology in secondary iron overload patients.[24] In this scenario, a healthcare provider would co-administer the transfusion and chelation therapy, and the sustained release of DFO-NP would ideally intercept iron as it is released from degraded RBCs and before it can be stored in organs. The model simulations show that a sustained release formulation would need to substantially reduce the absorption rate of DFO-NP by a factor of 5−10 in order to provide adequate exposure for a month. This could be accomplished by developing a formulation with minimal burst and pseudo-zero-order release to ensure that the absorption is adequately slowed. Injectable polymeric microparticles[25] or injectable hydrogels[26] are both formulation strategies that could reduce the absorption enough to enable a monthly dosing schedule. Regardless of the formulation used, a monthly dose would also require the use of a large-volume injection technology to ensure adequate drug is administered, and care should be taken to ensure the compatibility between these technologies.

Though these results are promising, they were limited by the reliance on theoretical estimates of allometric exponents (b = 1, 0.75, or −0.25). These exponents are most commonly used for simple allometric scaling when drug-specific parameters are not available due to the adherence to Kleiber's law relating metabolic rate and body weight via b = 0.75. However, there has been a long simmering debate about whether b = 0.67 is more appropriate to relate functions to body surface area instead of body weight.[13] Furthermore, others even dispute whether there can be a universal allometric exponent for different compounds and bolster this argument by citing the wide variety of published drug-specific exponents that range from 0.12 to 1.06 for clearance alone.[13,27] Therefore, in the future study, it will be important to establish DFO-NP-specific allometric exponents for all the mechanisms included in the PK model, especially those governing SC absorption, to improve the accuracy of prediction.

https://doi.org/10.1021/acsomega.3c02570
ACS Omega 2023, 8, 27256−27263

Another limitation of this work is the question of whether simple allometric scaling is suitable when dealing with nonlinear PK. This issue has been encountered when predicting the human PK of monoclonal antibodies (mAbs), which can show nonlinear PK due to multiple clearance mechanisms including target-mediated drug disposition (TMDD).[28] In these cases, the nonlinear noncompartmental parameters (e.g., clearance) cannot be directly scaled to humans. This issue was overcome for multiple therapeutic mAbs by using model-based analyses that incorporate Michaelis−Menten kinetics[29] or TMDD pathways[28,30] to model nonlinear elimination and then scaling these additional parameters. We have taken a similar approach for interspecies scaling of DFO-NP pharmacokinetics by using Michaelis−Menten kinetics to describe concentration-dependent (i.e., nonlinear) processes.

Collectively, the results of these experiments support the proposed use of SC bolus administration of DFO-NPs in a clinical setting. Additional PK studies should be conducted to improve the accuracy of the human PK prediction and thereby de-risk clinical development. Since the model suggests that there is significant lymphatic involvement, and since the model validation studies showed species-specific differences in lymph engagement, PK studies with direct lymph measurements would provide valuable data. Adequate lymph sampling could enable the development of a minimal physiologically-based model that may improve interspecies scaling. The PK of DFO-NPs should also be studied in large animals such as dog, sheep, or minipig. The minipig would be an ideal species for large animal PK, as pigs have the most similar SC characteristics to humans[31,34] and are expected to improve the accuracy of the model prediction. Another approach to improving model predictions would be to assess tissue distribution kinetics and develop a physiologically-based pharmacokinetic model which can include tissue-specific processes for lymphatic absorption and renal reabsorption.[32,35] Ultimately, the prediction of the human PK through allometric scaling suggests that DFO-NPs holds promise for further clinical development.

CONCLUSIONS

In the present study, model-based pharmacokinetic analysis of a novel iron chelating nanomedicine was expanded to novel species using allometric scaling. Model-based parameters were scaled down to mice and the nonlinear disposition and absorption models were validated for multiple doses. Model-based parameters were also scaled up to humans, and PK simulations were carried out to explore clinically relevant scenarios. These simulations demonstrated that (1) the favorable PK characteristics of DFO-NPs are expected to enable SC bolus injection in humans, which is expected to improve patient compliance over the typical SC infusion regimen of native DFO, (2) early clinical testing of DFO-NPs should proceed with daily administration of SC bolus injections, with a focus on optimizing formulation viscosity to ensure injectability, and (3) DFO-NP formulations that enable large-volume injections and incorporate sustained release technologies are expected to substantially improve drug exposure and meaningfully increase patient outcomes.

ASSOCIATED CONTENT

Supporting Information

The Supporting Information is available free of charge at https://pubs.acs.org/doi/10.1021/acsomega.3c02570.

Animal studies; pharmacokinetics of DFO-NP in mice after SC administration; blood sample processing; measurement of DFO-NP concentration; noncompartmental pharmacokinetic analysis (PDF)

AUTHOR INFORMATION

Corresponding Author

Jonghan Kim − *Department of Biomedical & Nutritional Sciences, University of Massachusetts Lowell, Lowell, Massachusetts 01854, United States;* orcid.org/0000-0001-8226-7427; Email: Jonghan_Kim@uml.edu

Authors

Gregory Jones − *Department of Pharmaceutical Sciences, Northeastern University, Boston, Massachusetts 02115, United States*

Lingxue Zeng − *Department of Biomedical & Nutritional Sciences, University of Massachusetts Lowell, Lowell, Massachusetts 01854, United States*

Complete contact information is available at: https://pubs.acs.org/10.1021/acsomega.3c02570

Notes

The authors declare no competing financial interest.

ACKNOWLEDGMENTS

This study was in part supported by the U.S. NIH/NHLBI HL143020 and HL163273 (J.K.).

REFERENCES

(1) Ganz, T. Systemic iron homeostasis. *Physiol. Rev.* **2013**, *93*, 1721−1741.

(2) Kohgo, Y.; Ikuta, K.; Ohtake, T.; Torimoto, Y.; Kato, J. Body iron metabolism and pathophysiology of iron overload. *Int. J. Hematol.* **2008**, *88*, 7−15.

(3) Murphy, C. J.; Oudit, G. Y. Iron-overload cardiomyopathy: pathophysiology, diagnosis, and treatment. *J. Card. Fail.* **2010**, *16*, 888−900.

(4) Gattermann, N. The treatment of secondary hemochromatosis. *Dtsch. Arztebl. Int.* 2009, *106* (30), 499−504, DOI: 10.3238/arztebl.2009.0499.

(5) Poggiali, E.; Cassinerio, E.; Zanaboni, L.; Cappellini, M. D. An update on iron chelation therapy. *J. Geophys. Res. Space Phys.* **2012**, *10*, 411−422.

(6) Hamilton, J. L.; Kizhakkedathu, J. N. Polymeric nanocarriers for the treatment of systemic iron overload. *Mol. Cell. Ther.* **2015**, *3*, 3.

(7) Jones, G.; Goswami, S. K.; Kang, H.; Choi, H. S.; Kim, J. Combating iron overload: a case for deferoxamine-based nanochelators. *Nanomedicine (Lond)* **2020**, *15*, 1341−1356.

(8) Kang, H.; Han, M.; Xue, J.; Baek, Y.; Chang, J.; Hu, S.; Nam, H.; Jo, M. J.; El Fakhri, G.; Hutchens, M. P.; et al. Renal clearable nanochelators for iron overload therapy. *Nat. Commun.* **2019**, *10*, 5134.

(9) Park, S. H.; Kim, R. S.; Stiles, W. R.; Jo, M.; Zeng, L.; Rho, S.; Baek, Y.; Kim, J.; Kim, M. S.; Kang, H.; Choi, H. S. Injectable Thermosensitive Hydrogels for a Sustained Release of Iron Nanochelators. *Adv. Sci.* **2022**, *9*, No. 2200872.

(10) Jones, G.; Zeng, L.; Stiles, W. R.; Park, S. H.; Kang, H.; Choi, H. S.; Kim, J. Pharmacokinetics and tissue distribution of deferoxamine-based nanochelator in rats. *Nanomedicine (Lond)* **2022**, *17*, 1649−1662.

(11) Jones, G.; Zeng, L.; Kim, J. Mechanism-Based Pharmacokinetic Modeling of Absorption and Disposition of a Deferoxamine-Based Nanochelator in Rats. *Mol. Pharmaceutics* **2023**, *20*, 481−490.

(12) Mahmood, I. Application of allometric principles for the prediction of pharmacokinetics in human and veterinary drug development. *Adv. Drug Deliv. Rev.* **2007**, *59*, 1177−1192.

(13) Mahmood, I. Theoretical Versus Empirical Allometry: Facts Behind Theories Application to Pharmacokinetics. *J. Pharm. Sci.* **2010**, *99*, 2927−2933.
(14) West, G. B.; Brown, J. H. The origin of allometric scaling laws in biology from genomes to ecosystems: towards a quantitative unifying theory of biological structure and organization. *J. Exp. Biol.* **2005**, *208*, 1575−1592.
(15) Bellanti, F.; Del Vecchio, G. C.; Putti, M. C.; Cosmi, C.; Fotzi, I.; Bakshi, S. D.; Danhof, M.; Della Pasqua, O. Model-Based Optimisation of Deferoxamine Chelation Therapy. *Pharm. Res.* **2016**, *33*, 498−509.
(16) Porter, J. B.; Rafique, R.; Srichairatanakool, S.; Davis, B. A.; Shah, F. T.; Hair, T.; Evans, P. Recent insights into interactions of deferoxamine with cellular and plasma iron pools: Implications for clinical use. *Ann. N. Y. Acad. Sci.* **2005**, *1054*, 155−168.
(17) Badkar, A. V.; Gandhi, R. B.; Davis, S. P.; LaBarre, M. J. Subcutaneous Delivery of High-Dose/Volume Biologics: Current Status and Prospect for Future Advancements. *Drug Des. Devel. Ther.* **2021**, *15*, 159−170.
(18) Turner, M. R.; Balu-Iyer, S. V. Challenges and Opportunities for the Subcutaneous Delivery of Therapeutic Proteins. *J. Pharm. Sci.* **2018**, *107*, 1247−1260.
(19) Swartz, M. A. The physiology of the lymphatic system. *Adv. Drug Deliv. Rev.* **2001**, *50*, 3−20.
(20) Porter, C. J.; Edwards, G. A.; Charman, S. A. Lymphatic transport of proteins after s.c. injection: implications of animal model selection. *Adv. Drug Deliv. Rev.* **2001**, *50*, 157−171.
(21) Berteau, C.; Filipe-Santos, O.; Wang, T.; Rojas, H. E.; Granger, C.; Schwarzenbach, F. Evaluation of the impact of viscosity, injection volume, and injection flow rate on subcutaneous injection tolerance. *Med. Devices (Auckl)* **2015**, *8*, 473−484.
(22) Frost, G. I. Recombinant human hyaluronidase (rHuPH20): an enabling platform for subcutaneous drug and fluid administration. *Expert Opin. Drug Deliv.* **2007**, *4*, 427−440.
(23) Locke, K. W.; Maneval, D. C.; LaBarre, M. J. ENHANZE drug delivery technology: a novel approach to subcutaneous administration using recombinant human hyaluronidase PH20. *Drug Deliv.* **2019**, *26*, 98−106.
(24) Origa, R. β-Thalassemia. *Genet. Med.* **2017**, *19*, 609−619.
(25) Anderson, J. M.; Shive, M. S. Biodegradation and biocompatibility of PLA and PLGA microspheres. *Adv. Drug Deliv. Rev.* **2012**, *64*, 72−82.
(26) Hoffman, A. S. Hydrogels for biomedical applications. *Adv. Drug Deliv. Rev.* **2012**, *64*, 18−23.
(27) Huh, Y.; Smith, D. E.; Feng, M. R. Interspecies scaling and prediction of human clearance: comparison of small- and macromolecule drugs. *Xenobiotica* **2011**, *41*, 972−987.
(28) Singh, R.; Moreno, M.; Stanimirovic, D. Comparison of Various Approaches to Translate Non-Linear Pharmacokinetics of Monoclonal Antibodies from Cynomolgus Monkey to Human. *Eur. J. Drug Metab. Pharmacokinet.* **2021**, *46*, 555−567.
(29) Wang, J.; Iyer, S.; Fielder, P. J.; Davis, J. D.; Deng, R. Projecting human pharmacokinetics of monoclonal antibodies from nonclinical data: comparative evaluation of prediction approaches in early drug development. *Biopharm. Drug Dispos.* **2016**, *37*, 51−65.
(30) Singh, A. P.; Krzyzanski, W.; Martin, S. W.; Weber, G.; Betts, A.; Ahmad, A.; Abraham, A.; Zutshi, A.; Lin, J.; Singh, P. Quantitative prediction of human pharmacokinetics for mAbs exhibiting target-mediated disposition. *AAPS J.* **2015**, *17*, 389−399.
(31) Mahl, J. A.; Vogel, B. E.; Court, M.; Kolopp, M.; Roman, D.; Nogués, V. The minipig in dermatotoxicology: Methods and challenges. *Exp. Toxicol. Pathol.* **2006**, *57*, 341−345.
(32) Dubbelboer, I. R.; Sjögren, E. Physiological based pharmacokinetic and biopharmaceutics modelling of subcutaneously administered compounds − An overview of in silico models. *Int. J. Pharm.* **2022**, *621*, No. 121808.
(33) Richter, W. F.; Bhansali, S. G.; Morris, M. E. Mechanistic Determinants of Biotherapeutics Absorption Following SC Administration. *AAPS J.* **2012**, *14*, 559−570.
(34) Richter, W. F.; Grimm, H.-P.; Gouy, M.-H.; Søgaard, S.; Kreuzer, C.; Wessels, U.; Draganov, D.; Muenzer, C.; Hoche, T. Subcutaneous Site-of-Absorption Study with the Monoclonal Antibody Tocilizumab in Minipigs: Administration Behind Ear Translates Best to Humans. *AAPS J.* **2020**, *22*, 63.
(35) Edginton, A. N.; Theil, F. P.; Schmitt, W.; Willmann, S. Whole body physiologically-based pharmacokinetic models: their use in clinical drug development. *Expert Opin. Drug Metab. Toxicol.* **2008**, *4*, 1143−1152.

https://doi.org/10.1021/acsomega.3c02570
ACS Omega 2023, 8, 27256−27263